Bispectral Analysis of High-Amplitude Jet Noise

Kent L. Gee*, Anthony A. Atchley†, Lauren E. Falco‡, Thomas B. Gabrielson§, and Victor W. Sparrow¶
The Pennsylvania State University, University Park, PA, 16802

The overall sound pressure levels of noise radiated by military jet aircraft along certain angles are such that nonlinearity is likely to influence the propagation. Bispectral analysis of noise data from the F/A-18E Super Hornet has been carried out in order to provide further evidence that nonlinear effects are indeed present. The bicoherence, which is a normalized form of the bispectral density, has been previously used in a variety of applications to detect quadratic phase coupling (QPC) in a signal. In this case, the results of the bicoherence calculations indicate that QPC is indeed present at high-thrust conditions along the peak radiation angles, which means that nonlinearity does play a role. However, additional investigations are still needed to more fully understand the physical interpretation of the bispectral results for a random noise signal, which will also help better quantify the role of nonlinearity in jet noise propagation.

Nomenclature

b	=	bicoherence
f	=	frequency (Hz)
f_s	=	sampling frequency (Hz)
M	=	number of ensembles
N	=	number of samples in time series
n_s	=	number of samples in each ensemble
S_{xx}	=	power spectral density (Pa^2/Hz)
S_{xxx}	=	bispectral density (Pa^3/Hz^2)
t	=	time (s)
T	=	total data record length (s)
w	=	windowing function
W	=	window equivalent noise bandwidth
x	=	time series variable (Pa)
X	=	Fourier transform of x (Pa/Hz)
Z	=	bifrequency spectral density (Pa^4/Hz^3)
Δt	=	time between samples or $1/f_s$ (s)
μ_x	=	mean (Pa)
σ_x^2	=	variance (Pa^2)
γ_x	=	skewness
$E[\,]$	=	expectation operator
*	=	complex conjugation operator
^	=	estimated quantity

* Ph.D. Candidate, Grad. Prog. in Acoustics, Penn State Univ., 202 Applied Science Bldg., University Park, PA 16802, kentgee@psu.edu, Student Member AIAA.
† Professor of Acoustics and Chair, Grad. Prog. in Acoustics, Penn State Univ., 217 Applied Science Bldg., University Park, PA 16802, Member AIAA.
‡ Ph.D. Candidate, Grad. Prog. in Acoustics, Penn State Univ., 202 Applied Science Bldg., University Park, PA 16802, Student Member AIAA.
§ Senior Research Associate, Applied Research Lab, Penn State Univ., P.O. Box 30, State College, PA 16804.
¶ Associate Professor of Acoustics, Grad. Prog. in Acoustics, Penn State Univ., 316B Leonhard Bldg., University Park, PA 16802, Senior Member AIAA.

I. Introduction

IN a previous work[1], evidence was shown that nonlinear effects were present in F/A-18E Super Hornet noise propagation at afterburner (AB) and military thrust (Mil) engine conditions. This paper presents results from a bispectral analysis of the data that provides additional confirmation that the propagation is nonlinear. As a finite-amplitude noise waveform propagates, Fourier spectral components interact in a quadratically nonlinear fashion to transfer energy to sum and difference frequencies. Although the bispectrum has proved a useful tool in analyzing data for quadratic nonlinearity in a variety of fields (e.g., see Refs. 2-5), it has not been previously applied to the identification of nonlinear effects in the propagation of high-amplitude jet noise.

This paper first introduces fundamental definitions and issues related to bispectral analysis in Sec. II, followed by a summary of the F/A-18E ground engine run-up measurements in Sec. III. Section IV contains comparisons of the bispectral results as a function of engine condition and measurement location, as well as relevant discussion, which is followed by some conclusions in Sec. V.

II. Overview of Bispectral Analysis

In the literature dedicated to the bispectrum and bispectral analysis, widely varying notation is used, some of which is inconsistent in terms of units and physical meaning. Therefore, one purpose of this section is to provide a physically consistent development of the bispectrum, for both continuous and discrete processes. In addition, one particular bispectral normalization known as the bicoherence[6] is discussed in some detail with regards to physical interpretation and digital estimation issues.

A. The Bispectrum

For the sake of clarity, it is first helpful to review the definition and physical significance of the power spectral density (PSD) before proceeding to a development of the bispectrum. For a zero-mean acoustic pressure signal, $x(t)$, expressed in pascals (Pa), the PSD is given as

$$S_{xx}(f) = \lim_{T\to\infty} \frac{1}{T} E\left[X(f)X^*(f)\right]. \tag{1}$$

In Eq. (1), $X(f)$ is the Fourier transform of $x(t)$, which may be expressed as

$$X(f) = \int_{-\infty}^{\infty} x(t)e^{-j2\pi ft}dt\,, \tag{2}$$

$E[\ ]$ is the expectation operator, and T is record length. Because $X(f)$ has units of Pa/Hz, the units of $S_{xx}(f)$ in Eq. (1) are Pa^2/Hz. The PSD decomposes the power contained in $x(t)$ as a function of frequency, where the signal power is equal to the mean-square value or variance, σ_x^2, of the signal. Therefore, $S_{xx}(f)$ may be integrated as

$$\sigma_x^2 = E\left[x^2(t)\right] = \int_{-\infty}^{\infty} S_{xx}(f)df \tag{3}$$

to yield σ_x^2, which is both the second-order moment and cumulant[7] of $x(t)$. In general, the mth-order cumulant and moment of a signal are not equal (e.g., see the discussion in Ref. 8). However, the distinction is unimportant in this case because they are equal up to and including $m = 3$, the highest order considered in this paper. Because of its relationship to σ_x^2, $S_{xx}(f)$ is also known as the second-order cumulant spectrum[7,8]. Note that in much of the literature dedicated to polyspectra, $S_{xx}(f)$ is simply identified as the power spectrum, rather than the power spectral density. However, because of the units associated with $S_{xx}(f)$, it is more appropriately labeled as a spectral density.

The bispectral density (BSD) is the third-order cumulant spectrum, which is defined as

$$S_{xxx}(f_1, f_2) = \lim_{T\to\infty} \frac{1}{T} E\left[X(f_1)X(f_2)X^*(f_1 + f_2)\right], \tag{4}$$

and has units of Pa^3/Hz^2. Just as $S_{xx}(f)$ decomposes the variance of the signal, $S_{xxx}(f_1, f_2)$ decomposes the third-order cumulant of the signal, $E\left[x^3(t)\right]$, at a given (f_1, f_2) or bifrequency. This relationship is expressed mathematically as

$$E\left[x^3(t)\right] = \int_{-\infty}^{\infty}\int_{-\infty}^{\infty} S_{xxx}(f_1, f_2)\,df_1 df_2 . \tag{5}$$

Because the skewness, or normalized third-order moment of the signal, is defined as

$$\gamma_x = \frac{E\left[x^3(t)\right]}{\left(\sigma_x^2\right)^{3/2}}, \tag{6}$$

the BSD provides a measure of γ_x as a function of frequency. Additionally, due to regions of bispectral symmetry[8] in the bifrequency plane, only the real part of the BSD contributes to $E\left[x^3(t)\right]$. Finally, note that the term "bispectral density" is somewhat uncommon—instead, Eq. (4) is usually referred to simply as the "bispectrum." However, similar to the preceding discussion regarding the PSD, the so-called bispectrum is more appropriately identified as a spectral density; therefore, $S_{xxx}(f_1, f_2)$ in Eq. (4) is referred to as the BSD in this paper.

For a statistically Gaussian signal, the BSD and all higher-order spectra are zero; therefore a non-zero BSD calculation is an indicator that a signal is non-Gaussian and possibly nonlinear. Bispectral analysis can be further used to detect the presence of quadratic phase coupling (QPC) in a signal. QPC indicates that second-order nonlinearity is present in the system, resulting in an interaction of power spectral components at f_1 and f_2 to transfer energy to $f_1 + f_2$ and $f_1 - f_2$, which are respectively known as the sum and difference frequencies. However, the difficulty of using the BSD directly to detect QPC is that, in practice, the variance of the $S_{xxx}(f_1, f_2)$ estimate is dependent on the PSD shape and amplitude, as well as the strength of QPC[6] in the signal. To address this problem, normalizations[5,7] of the BSD have been proposed.

B. The Bicoherence

One normalization for the BSD, developed by Kim and Powers[8], is known as the bicoherence. The bicoherence, $b(f_1, f_2)$, has been frequently used to identify QPC between power spectral components in a variety of applications. The bicoherence may be defined as

$$b(f_1, f_2) = \frac{\left|S_{xxx}(f_1, f_2)\right|}{\sqrt{Z(f_1, f_2)S_{xx}(f_1 + f_2)}}, \tag{7}$$

where the bifrequency spectral density, $Z(f_1, f_2)$, is defined as

$$Z(f_1, f_2) = \lim_{T\to\infty} \frac{1}{T} E\left[\left|X(f_1)X^*(f_2)\right|^2\right]. \tag{8}$$

The bicoherence is bounded between 0 and 1, which may be understood by first expressing $b(f_1, f_2)$ in a simplified form as

$$b(f_1, f_2) = \frac{\left| E\left[X(f_1)X(f_2)X^*(f_1+f_2)\right]\right|}{\sqrt{E\left[\left|X(f_1)X(f_2)\right|^2\right]E\left[\left|X(f_1+f_2)\right|^2\right]}} \tag{9}$$

and then applying the Cauchy-Schwarz inequality

$$\left| E[\alpha\beta] \right|^2 \le E\left[|\alpha|^2\right]E\left[|\beta|^2\right] \tag{10}$$

to $b(f_1, f_2)$, where $\alpha = X(f_1)X(f_2)$ and $\beta = X(f_1 + f_2)$. The bounds of $b(f_1, f_2)$ can be useful in providing an interpretation to a given calculation. Discussion of the bicoherence interpretation, however, is delayed until after the next subsection, which treats the estimation of the BSD and bicoherence for a discrete process.

C. Digital Bispectrum Estimation

The discussion up to this point has been in terms of the continuous representations of $x(t)$ and other variables, primarily to establish the correct physical units associated with the various quantities. Estimation of the BSD and bicoherence for a digitally-sampled signal involves other considerations that are now discussed. First of all, due to the regions of symmetry for the continuous bispectrum and the periodic nature of discrete Fourier transforms (DFT), the principal domain of the BSD estimate is the triangular region defined by $0 \le f_2 \le f_1$ and $f_2 + f_1 = f_s/2$, where f_s is the sampling frequency of the data [8]. There are various means of carrying out the calculation of the BSD and bicoherence estimates, which will be denoted as $\hat{S}_{xxx}(f_1, f_2)$ and $\hat{b}(f_1, f_2)$, respectively. From several bispectral processing techniques reviewed by Nikias and Petropulu[8], the method used to calculated the results presented subsequently is a simple ensemble-averaging method. First, a time series that is N samples in length, where N is a power of two, is divided into M ensembles each consisting of n_s samples. The length of each ensemble is chosen to be

$$n_s = 2^{\left\lceil \log_2\left(\sqrt{N}\right)\right\rceil}, \tag{11}$$

where $\lceil\ \rceil$ is the ceiling operator, which essentially combines the recommendation by Dalle Molle and Hinich[9] that the ensemble length be $\sqrt{N}$ and the desire that n_s be a power of two for efficient processing. For $N = 2^{19}$, application of Eq. (11) results in $n_s = 2^{10}$; however, note that using $n_s = 2^9$ and $n_s = 2^{11}$ did not change calculated results appreciably.

Based on the recommendation of Nikias and Petropulu[8], a Hamming window is applied to the data, with an overlap of 50% between individual ensembles, to reduce spectral leakage. Although a Hanning window is more commonly used in the spectral analysis of noise signals, this window is not an appropriate choice for bispectral analysis because it has negative side lobes in the frequency domain[8].

After each ensemble has been windowed, $\hat{S}_{xx}(f)$ and $\hat{S}_{xxx}(f_1, f_2)$ may be calculated via an extension of the Welch periodogram method (e.g., see Refs. 8 and 10). If the discrete-time Fourier transform (DTFT)[10] of the mth ensemble is defined as

$$\hat{X}^{(m)}(f) = \Delta t \sum_{n=0}^{n_s-1} x^{(m)}[n] e^{-j2\pi f n \Delta t}, \tag{12}$$

where n is the sample index, then $\hat{S}_{xx}(f)$ may be calculated on a windowed ensemble, $x_w^{(m)}$, as

$$\hat{S}_{xx}(f) = \frac{1}{M}\sum_{m=1}^{M} \frac{1}{n_s \Delta t W}\left|\hat{X}_w^{(m)}(f)\right|^2, \tag{13}$$

where W is the equivalent noise bandwidth of the windowing function, w, calculated as

$$W = \frac{1}{n_s}\sum_{n=0}^{n_s-1} w^2[n]. \tag{14}$$

Likewise, $\hat{S}_{xxx}(f_1, f_2)$ is calculated as

$$\hat{S}_{xxx}(f_1, f_2) = \frac{1}{M}\sum_{m=1}^{M} \hat{S}_{xxx}{}^{(m)}(f_1, f_2), \tag{15}$$

where

$$\hat{S}_{xxx}{}^{(m)}(f_1, f_2) = \frac{1}{n_s \Delta t W^{3/2}}\left[\hat{X}^{(m)}(f_1)\hat{X}^{(m)}(f_2)\hat{X}^{(m)}(f_1 + f_2)\right]. \tag{16}$$

Once $\hat{Z}(f_1, f_2)$ has been calculated in similar fashion as the PSD estimate in Eq. (13), $\hat{b}(f_1, f_2)$ may be computed as

$$\hat{b}(f_1, f_2) = \frac{1}{M}\sum_{m=1}^{M} \frac{\left|\hat{S}_{xxx}{}^{(m)}(f_1, f_2)\right|}{\sqrt{\hat{Z}(f_1, f_2)\hat{S}_{xx}(f_1 + f_2)}}. \tag{17}$$

Alternatively, the bicoherence estimate may be calculated directly from Eq. (9) using the DTFT in Eq. (12) or the discrete Fourier transform.

Because $\hat{S}_{xxx}(f_1, f_2)$ and $\hat{b}(f_1, f_2)$ will generally be slightly non-zero for even Gaussian series of finite length, it is worthwhile to consider threshold levels of statistical significance. Elgar and Guza[11] numerically investigated the statistical properties of $\hat{b}(f_1, f_2)$ as a function of number of ensembles, M, for non-overlapping (non-windowed) Gaussian time series. They found good agreement between numerical calculations of significance levels and theoretical predictions based on an assumed chi-square distribution for $\hat{b}^2(f_1, f_2)$. For the 99% confidence level and large M, the threshold of significant bicoherence was found to follow $\sqrt{4.6/M}$, meaning that any $\hat{b}(f_1, f_2)$ value below that threshold is not statistically significant. There is some uncertainty as to how to apply their result to the present research because Elgar and Guza[11] did not window and overlap their data segments, as has been done in this analysis. However, use of the non-overlapped number of ensembles, $M = N/n_s$, in the Elgar and Guza result yields a conservative estimate for the 99% level threshold of significant bicoherence of approximately 0.095 for $N/n_s = 512$.

D. Physical Interpretation of the Bicoherence

As previously discussed, the BSD can be used to identify quadratic nonlinearity in a system. The bicoherence provides a measure of the degree to which QPC exists among spectral components in a signal, but currently has a strict quantitative interpretation only if that signal is periodic. For a periodic signal with spectral components at f_1, f_2, and $f_1 + f_2$, calculation of $\hat{b}(f_1, f_2)$ yields the fraction of power at $f_1 + f_2$ that is present due to QPC[6]. If the component at $f_1 + f_2$ exists only because of a nonlinear interaction between f_1 and f_2, then $\hat{b}(f_1, f_2) \to 1$. Unfortunately, for a nonlinear random noise signal, multiple bifrequencies may interact nonlinearly to yield a single component of $\hat{S}_{xx}(f)$. There is a cascading of sum and difference frequency generation that makes quantitative

analysis of a bicoherence spectrum difficult. Greb and Rusbridge[12] have investigated broadband spectral interactions in the context of nonlinear plasma physics and have found that the maximum value of $\hat{b}(f_1, f_2)$ may be reduced in an ill-defined manner which depends on both spectral shape and resolution. They suggest that although the bicoherence is only useful for rather coarse spectral resolution, it is nevertheless helpful because its normalization allows the identification of nonlinear coupling that is undetectable with $S_{xxx}(f_1, f_2)$. Recently, Hinich and Wolinsky[13] have criticized the Kim and Powers[6] normalization by demonstrating that $Z(f_1, f_2)$ can be shown to depend upon both the spectral resolution and upon the next higher-order spectrum, the trispectral density. They instead promote the use of a different normalization, originally formulated by Haubrich[5] and later termed the skewness function[14], which is defined as

$$\hat{s}(f_1, f_2) = \frac{\left| E\left[X(f_1)X(f_2)X^*(f_1+f_2)\right]\right|}{\sqrt{E\left[\left|X(f_1)\right|^2\right]E\left[\left|X(f_2)\right|^2\right]E\left[\left|X(f_1+f_2)\right|^2\right]}}. \tag{19}$$

Unlike the bicoherence, there is no upper bound on $\hat{s}(f_1, f_2)$; however, its variance is flat as a function of bifrequency, which allows signal linearity to be readily determined via a statistical test based on a chi-square distribution assumption. Although only $\hat{b}(f_1, f_2)$ results are presented in this paper, $\hat{s}(f_1, f_2)$ was also calculated using Eq. (19), yielding very similar results. Therefore, in this application of bispectral analysis to identify nonlinearity in high-amplitude jet noise, the bicoherence normalization is likely sufficient, because conclusions are currently based on relative comparisons between measurement locations and engine conditions.

III. F/A-18E Measurement Summary

Static engine run-up tests were conducted on the F/A-18E Super Hornet at NAVAIR Lakehurst, NJ during the evening of 15 April 2003. Recordings of the noise radiated with both engines at idle, military thrust (Mil) and with afterburners (AB) engaged were made with Sony TCD-D8 digital audio tape recorders sampling at 44.1 kHz. From each recording, 524,288 (2^{19}) samples or approximately 11 s of data were used for these analyses. Data were collected at 18, 74, and 150 m from the engine nozzles and at various angles, as shown in Figure 1. The 18 m data were acquired with a Bruel & Kjaer 4938 6.35-mm (¼-in) condenser microphone flush-mounted in an aluminum plate baffle located horizontally on pavement. The 74 and 150 m data were acquired with handheld Endevco 8510C-15 piezoresistive pressure transducers located about 1.2 m above grassy ground. Significant multipath effects are present in the PSD measurements at 74 m and 150 m, which are likely due, at least partially, to terrain inhomogeneity over the measurement range. The power spectral measurements along 135°, which is approximately the peak directivity angle at high-thrust conditions and where nonlinearity is most likely to occur, have been analyzed and discussed previously[1]. Although the PSD measurements at the remaining data collection locations are not shown in this paper due to its focus on bispectral analysis, the measured overall sound pressure level (OASPL) at each of the locations and engine conditions is shown in Table 1. It is perhaps noteworthy that while the OASPL at 74 m monotonically increases as a function of angle, the same is not true for 150 m, where the overall levels at 120-135° are approximately equal for both AB and Mil.

Table 1. Overall sound pressure level (OASPL, dB re 20 µPa) as a function of distance, angle and engine condition, shown as AB / Mil / idle. At idle, only the 18 m measurement is shown; all other idle measurements are largely or completely below the system noise floor. An asterisk (*) is used to indicate cases for which the measured power spectral density reaches the noise floor below 10 kHz, but at a frequency (e.g., 5-6 kHz) such that the OASPL is unlikely to be affected significantly.

	135°	130°	120°	105°	90°
18 m	151 / 147 / 99*	--	--	--	--
74 m	135 / 132	134 / 128	128 / 124	123 / 120	--
150 m	127 / 123	128 / 124	127 / 123	116* / 110*	114* / 108*

IV. Results and Discussion

In this section, a variety of bicoherence results are presented and discussed. First, however, some comments regarding the maximum calculated bifrequency are worthwhile. Because the DAT recorders used in the measurements sample the radiated pressure waveform at f_s = 44.1 kHz, the theoretical principal domain is substantially larger than what will be shown. There are two reasons for truncating the domain; first of all, only bifrequencies (f_1, f_2) for which $\hat{S}_{xx}(f_1 + f_2)$ is above the system noise floor are shown. This condition affects those measurements for which the OASPL in Table 1 is marked with an asterisk. Second, an experimentally-measured amplitude diffraction correction was applied to the piezoresistive sensor measurements because of the sensor housing design. Uncertainty in this diffraction correction above 10 kHz resulted in questionable PSD levels above that frequency, even if above the noise floor. In principle, calculation of $\hat{b}(f_1, f_2)$ results in a cancellation of the pressure amplitude diffraction correction, which would allow the range of the bispectral analysis to be extended beyond $f_1 + f_2$ = 10 kHz. However, in practice, the diffraction around the housing for the Endevco sensor would affect not only the measured amplitude but the phase of the Fourier pressure spectrum components, which would, in turn, influence the observed degree of QPC. Because the sensor diffraction correction for phase is currently unknown, $f_1 + f_2$ has been limited to below 10 kHz for this analysis.

A. Engine Condition Comparison at 18 m

The calculated $\hat{b}(f_1, f_2)$ at 18 m is shown in Figs. 2-4 for AB, Mil, and idle, respectively. The levels of bicoherence in Fig. 2 for AB are well above the threshold of significance of 0.095 above approximately 200 Hz on the ordinate, indicating that nonlinear interactions between frequencies are occurring. In other words, waveform steepening is resulting in energy transfer from the peak frequency region of the spectrum, which is around 200-300 Hz, to higher frequencies. Note that because $\hat{b}(f_1, f_2)$ is essentially zero (i.e., below the threshold) for ordinate frequencies below 200 Hz, nonlinear energy transfer to lower frequencies via difference frequency generation is not significant at this distance.

Figure 3 for Mil power at 18 m is qualitatively similar to Fig. 2 for AB; however, the bicoherence levels in Fig. 3 are generally lower, suggesting that while nonlinear effects are also present at Mil power, they are relatively less significant. On the other hand, in Fig. 4 for idle, there is no evidence of QPC; in fact, $\hat{b}(f_1, f_2)$ is statistically insignificant for virtually all bifrequencies. In effect, the idle results in Fig. 4 yield a baseline case for linearity in this paper, to which all other results may be compared.

B. Angular Variation Comparison at 74 m

Given the results in the previous subsection, it is expected that nonlinearity should be the greatest at AB. The bicoherence was calculated for this engine condition for the all the angles at 74 m. As might be expected, the $\hat{b}(f_1, f_2)$ levels follow the same trend as the OASPL, which increases as a function of angle. The bicoherence results for 135°, 120°, and 105° are shown in Figs. 5-7, respectively. The amount of QPC is minimal at 120° and nonexistent at 105°. Before moving on to the results at 150 m, some discussion of the deep nulls that occur in the $\hat{b}(f_1, f_2)$ in Fig. 5 is needed. These nulls occur because of the multipath interference phenomena that are especially present in the 74 m PSD measurements[1]. Fackrell *et al.*[15] have discussed the behavior of bicoherence for frequency regions in which there is very little signal power. Theoretically, in these regions $\hat{b}(f_1, f_2)$ would equal 0/0; however, in practice, the ensemble-averaged bispectral estimate, which is in the numerator, will approach zero, while the quantities in the denominator will not, since they are limited by the magnitude of the measurement system noise floor. The result is that $\hat{b}(f_1, f_2)$ also approaches zero in these regions. For example, if there is a sharp null in a PSD measurement at f_{null}, then nulls will exist in $\hat{b}(f_1, f_2)$ along (f_1, f_{null}), (f_{null}, f_2), and $(f_1, f_{null} - f_1)$, which comprise lines parallel, perpendicular, and 45º to the abscissa. In the measured PSD at 74 m, there is a broad null between 400-800 Hz, and then subsequent nulls appear approximately every 600-700 Hz[1]. The effects of these nulls can be seen in Fig. 5, severely contaminating the bicoherence measurements.

Despite the issues created by the interference effects, at those frequencies not influenced by the nulls, the bicoherence levels in Fig. 5 are still substantially above the significance threshold, indicating that nonlinear coupling is still present. In addition, one significant feature of Fig. 5 that differs from $\hat{b}(f_1, f_2)$ for AB at 18 m is that there

appears to be energy transfer downward in the spectrum because there is an indication of QPC at low ordinate frequencies. This would indicate that difference frequency generation influences the propagation at 74 m.

C. Angular Variation Comparison at 150 m

Although a comparison of the AB bicoherence at 74 m as a function of angle has already been carried out, it is worthwhile to do the same at 150 m because of the different trends in OASPL noted previously. In Figs. 8-10, $\hat{b}(f_1, f_2)$ for AB at 150 m and 135°, 120°, and 105° are displayed. The multipath interference effects are not as substantial at 150 m (i.e., the PSD nulls are not as deep); consequently, there are fewer nulls in the bicoherence. Comparison of the Figs. 8 and 9 at 150 m with Figs. 5 and 6 at 74 m show distinctly the presence of QPC at 150 m and 120° that was not apparent at 74 m. In light of the OASPL results in Table 1, the presence of QPC at 120° and 150 m but not at 74 m is perhaps not unexpected; however, the reason for it remains unknown at this point. One possible cause (though this is unlikely to be the only contributor) is the finite extent of the jet noise source. Because the effective aeroacoustic source is not located at the nozzle, but instead several meters downstream, if the Mach wave angle is somewhat less than 120°, the propagation could cross the radials depicted in Fig. 1 and result in high levels at 150 m and 120° but not at 74 m. This comment is speculative and other factors such as ground and meteorological effects very likely play a role in this case. However, despite this apparent anomaly, a comparison of Figs. 8 and 9 with Fig. 2 at 18 m suggests that QPC is diminishing at 150 m, which may indicate that the net effect of propagation through turbulence, wind, and over finite-impedance terrain is a reduction of the phase-coupled relationship between spectral components.

V. Conclusion

This initial investigation of bispectral analysis of jet noise propagation has yielded evidence of quadratic phase coupling (QPC) at high-thrust conditions along peak radiation angles where nonlinear effects would be most likely. The presence of QPC demonstrates that the propagation is, in fact, inherently nonlinear. However, additional work is needed to better understand, from a quantitative standpoint, the physical significance of the bicoherence for a propagating finite-amplitude random noise waveform. For that reason, controlled propagation experiments in a one-dimensional duct are planned that will investigate the effects of waveform amplitude, frequency content, and statistics on the evolution of the bispectral density and its normalizations. These experiments will help quantify the degree to which nonlinearity influences the propagation of high-amplitude jet noise.

Acknowledgments

The authors would like to thank Dr. Robert Keolian of Penn State for bringing to their attention the potential utility of the bispectrum in jet noise analysis. The authors also gratefully acknowledge the cooperation of Richard McKinley, the Air Force Research Laboratory, and their respective research sponsors. A. A. Atchley and T. B. Gabrielson are supported by the Office of Naval Research. K. L. Gee and V. W. Sparrow are funded by the Strategic Environmental Research and Development Program, as a subcontract through Wyle Laboratories, Arlington, VA. L. E. Falco is supported by a Graduate Research Fellowship through the National Science Foundation.

References

[1]Gee, K. L., Gabrielson, T. B., Atchley, A. A., Sparrow, V. W., "Preliminary Analysis of Nonlinearity in F/A-18E/F Noise Propagation," AIAA paper 2004-3009, May 2004.

[2]Brockett, P. L., Hinich, M., and Wilson, G. R., "Nonlinear and Non-Gaussian Ocean Noise," *Journal of the Acoustical Society of America*, Vol. 82, No. 4, 1987, pp. 1386-1394.

[3]Norris, J. D. and Chokani, N., "Transonic Nonlinear Interactions in a Hypersonic Boundary Layer," AIAA paper 2002-0154, Jan. 2002.

[4]Fackrell, J. W. A. and McLaughlin, S., "The Higher-order Statistics of Speech Signals," *IEE Colloquium (Digest)*, No. 138, 1 June 1994, pp. 7/1-7/6.

[5]Haubrich, R. A., "Earth Noise, 5 to 500 Millicycles per Second," *Journal of Geophysical Research*, Vol. 70, No. 6, 1965, pp. 1415-1427.

[6]Kim, Y. C. and Powers, E. J., "Digital Bispectral Analysis and its Applications to Nonlinear Wave Interactions," *IEEE Transactions on Plasma Science*, Vol. PS-7, No. 2, 1979, pp. 120-131.

[7]Brillinger, D. R., "An Introduction to Polyspectra," *The Annals of Mathematical Statistics*, Vol. 36, No. 5, 1965, pp. 1351-1374.

[8]Nikias, C. L. and Petropulu, A. P., *Higher-order Spectra Analysis: A Nonlinear Signal Processing Framework*, Prentice Hall, Upper Saddle River, NJ, 1993.

[9]Dalle Molle, J. W. and Hinich, M. J., "The Trispectrum," *Proceedings of the Workshop on Higher Order Spectral Analysis*, Vail, CO, 1989, pp. 68-72.
[10]Marple, S. J., *Digital Spectral Analysis with Applications*, Prentice Hall, Upper Saddle River, NJ, 1987.
[11]Elgar, S. and Guza, R. T., "Statistics of Bicoherence," *IEEE Transactions on Acoustics, Speech, and Signal Processing*, Vol. 36, No. 10, 1988, pp. 1667, 1668.
[12]Greb, U. and Rusbridge, M. G., "The Interpretation of the Bispectrum and Bicoherence for Non-linear Interactions of Continuous Spectra," *Plasma Physics and Controlled Fusion*, Vol. 30, No. 5, pp. 537-549.
[13]Hinich, M. J. and Wolinsky, M., "Normalizing Bispectra," *Journal of Statistical Planning and Inference*, Vol. 130, 2005, pp. 405-411.
[14]Hinich, M. J., "Testing for Gaussianity and Linearity of a Stationary Time Series," *Journal of Time Series Analysis*, Vol. 3, No. 3, 1982, pp. 169-176.
[15]Fackrell, J. W., White, P. R., Hammond, J. K., Pinnington, R. J., and Parsons, A. T., "The Interpretation of the Bispectra of Vibration Signals—I. Theory," *Mechanical Systems and Signal Processing*, Vol. 9, No. 3, 1995, pp. 257-266.

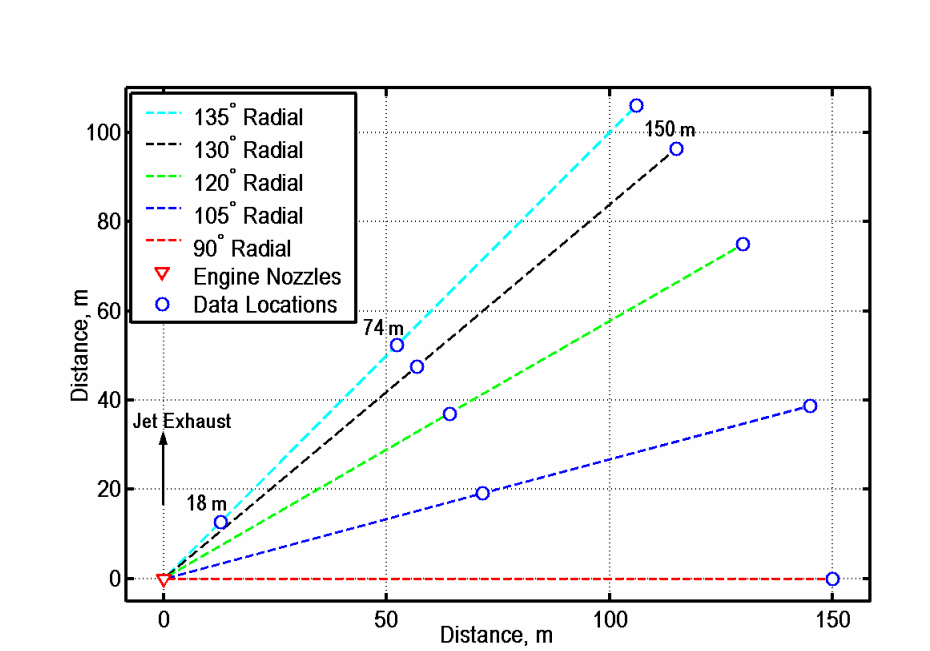

Figure 1. Engine run-up measurement layout. The angles are measured relative to the jet axis from the forward direction.

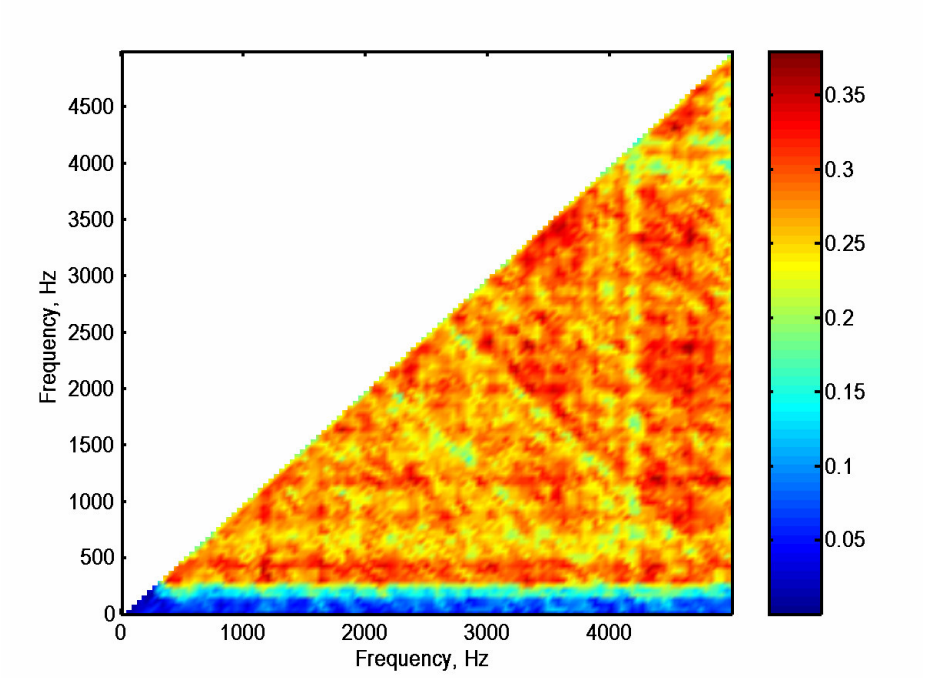

Figure 2. Bicoherence at 18 m for AB.

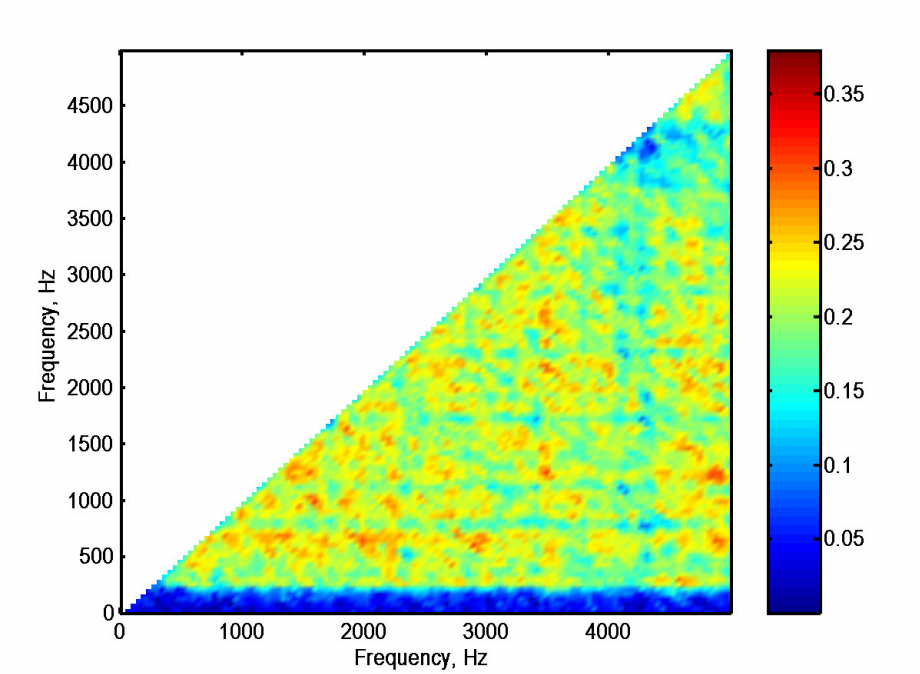

Figure 3. Bicoherence at 18 m for Mil.

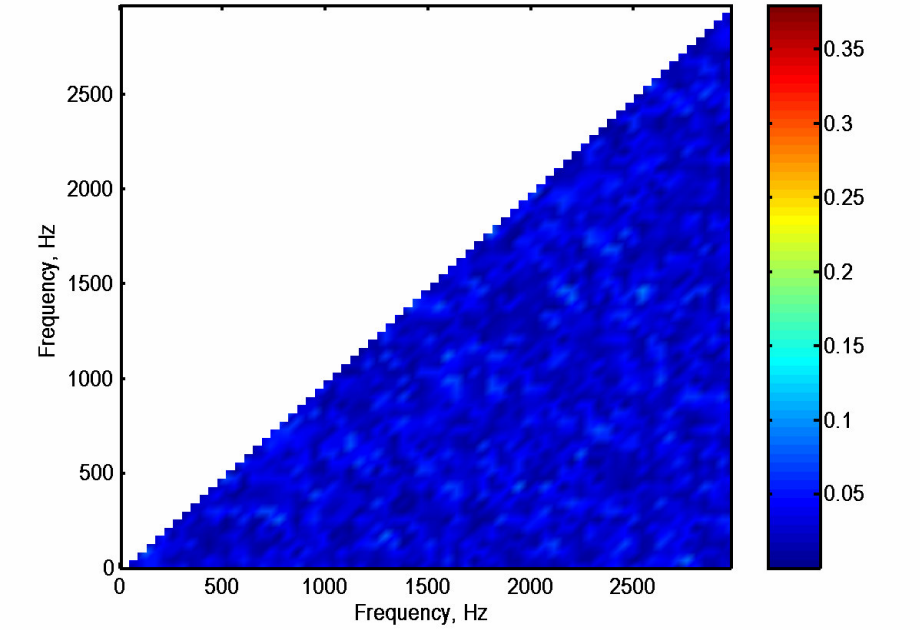

Figure 4. Bicoherence at 18 m for idle.

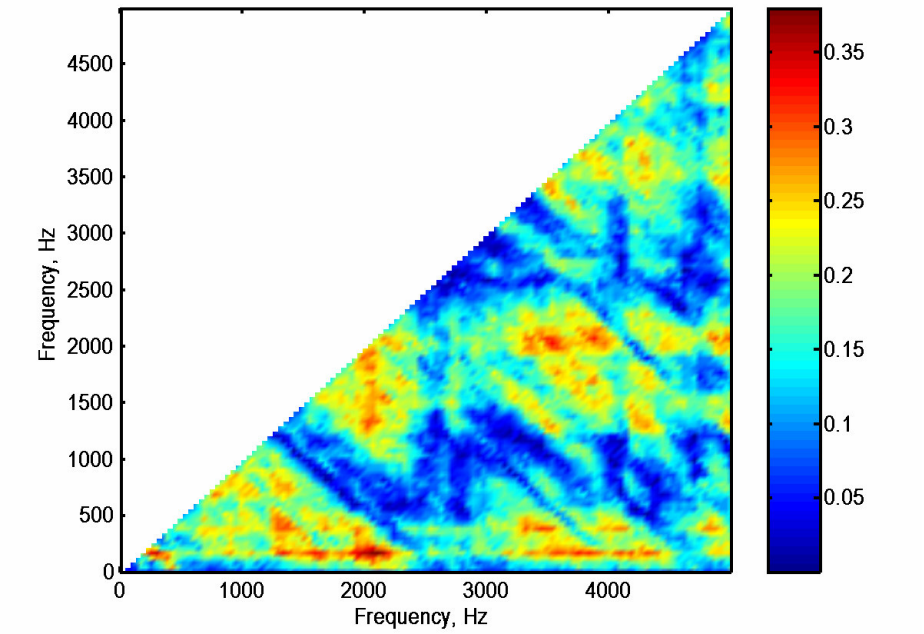

Figure 5. Bicoherence at 74 m, 135° for AB.

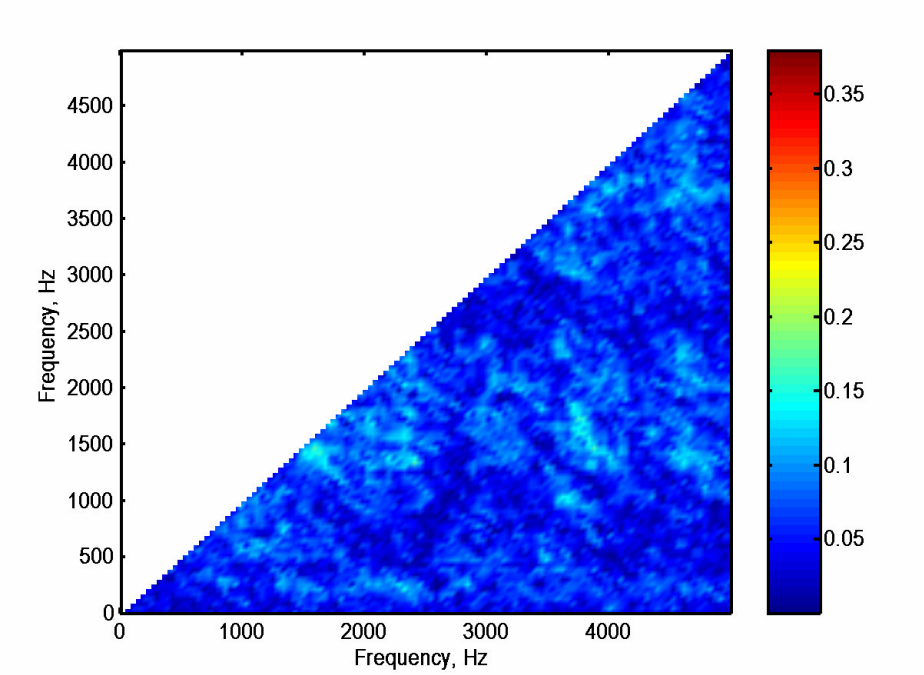

Figure 6. Bicoherence at 74 m, 120° for AB.

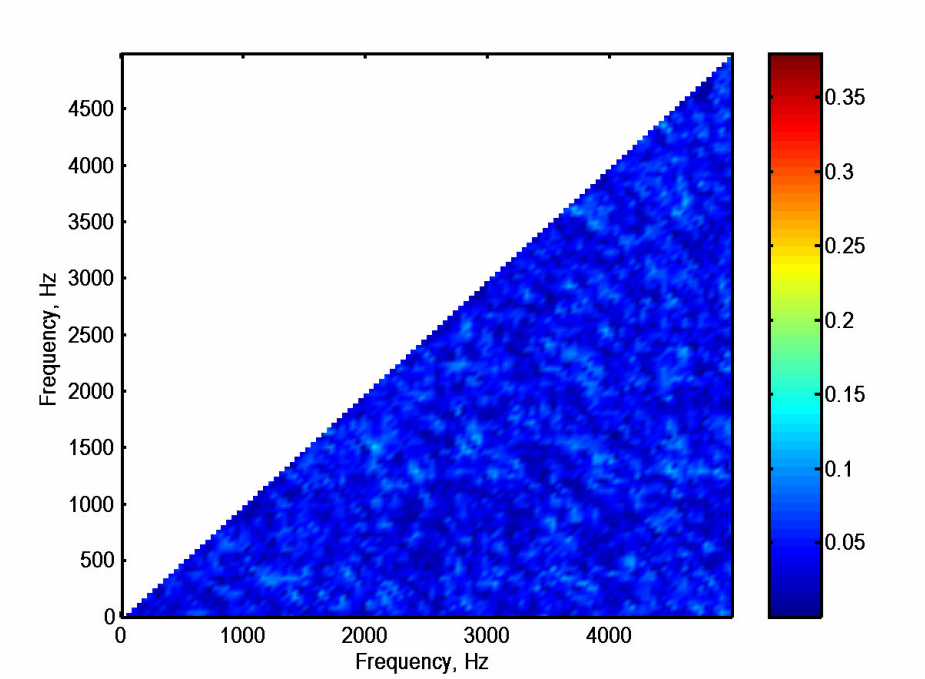

Figure 7. Bicoherence at 74 m, 105° for AB.

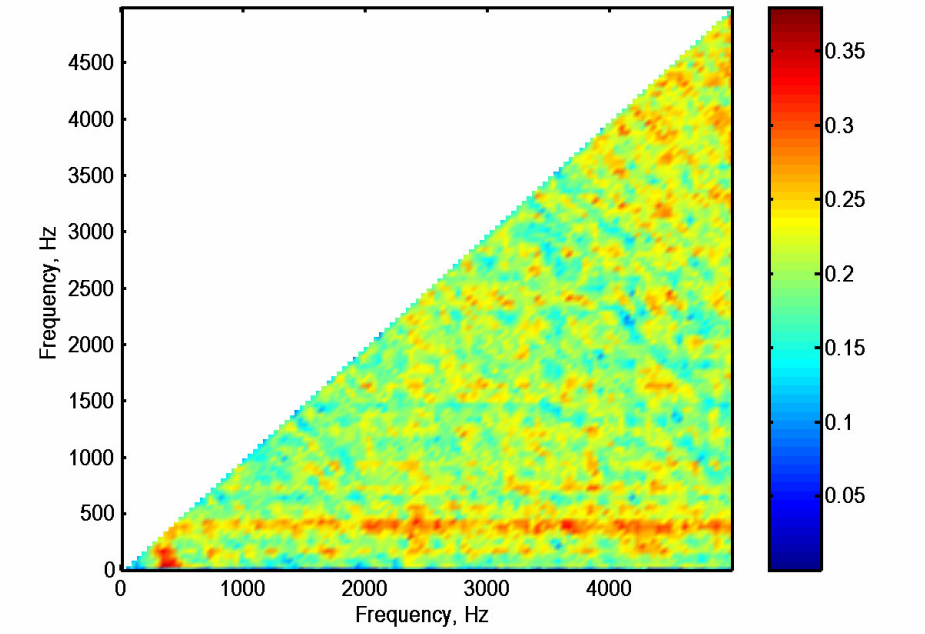

Figure 8. Bicoherence at 150 m, 135° for AB.

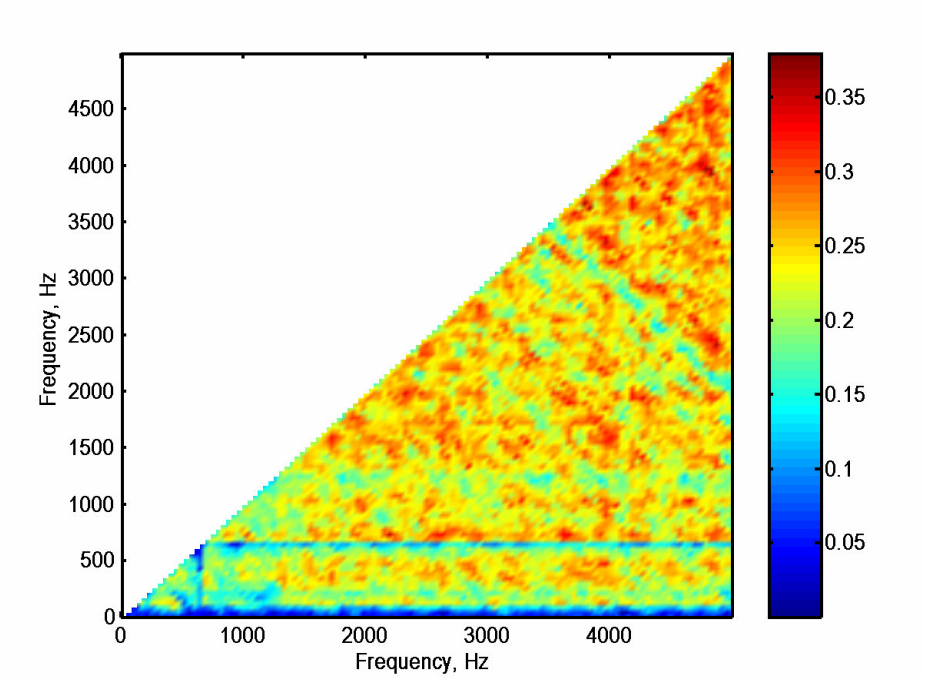

Figure 9. Bicoherence at 150 m, 120° for AB.

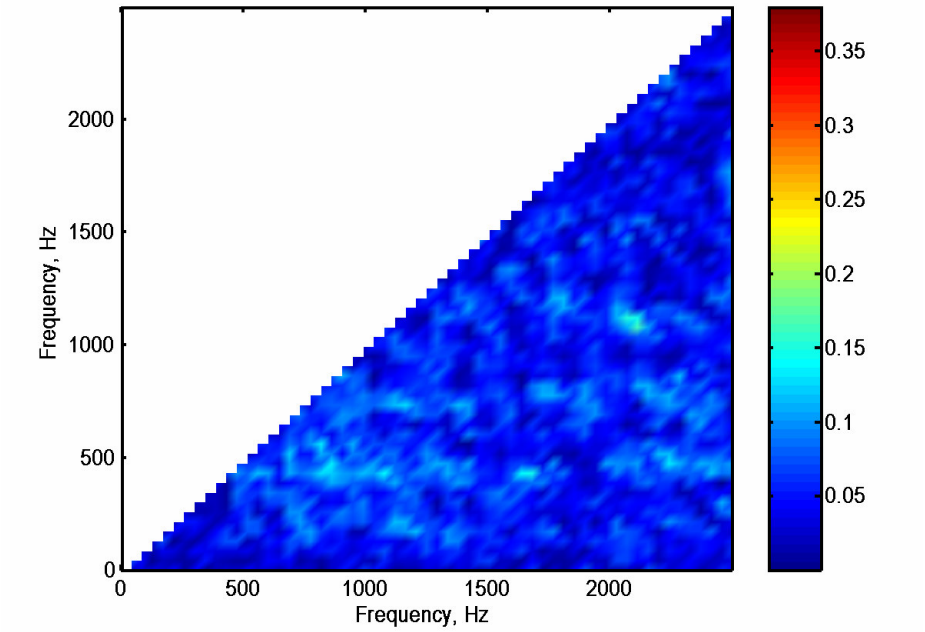

Figure 10. Bicoherence at 150 m, 105° for AB.